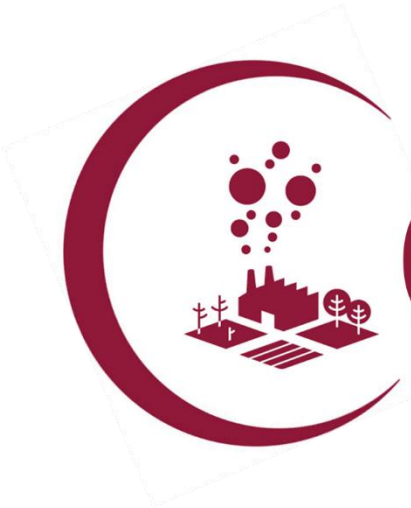

CONFESS

Consistent representation of temporal variations of boundary forcings in reanalyses and seasonal forecasts

D2.4 Validation report on the experiments using biomass burning climatological and observed emissions.

Roberto Bilbao (BSC), Elisabet Sorribes (BSC), Angela Benedetti (ECMWF), Etienne Tourigny (BSC), Pablo Ortega (BSC), Frederic Vitart (ECMWF) and Magdalena A. Balmaseda (ECMWF)

www.confess-h2020.eu

CONFESS

Consistent representation of temporal variations of boundary forcings in reanalyses and seasonal forecasts

D2.4 Validation report on the experiments using biomass burning climatological and observed emissions for the selected test cases

Author(s): Roberto Bilbao (BSC), Elisabet Sorribes (BSC), Angela Benedetti (ECMWF), Etienne Tourigny (BSC), Pablo Ortega (BSC), Frederic Vitart (ECMWF), Magdalena A. Balmaseda (ECMWF)

Dissemination Level: Public

Date: 30/06/2023

Version: 0.1

Contractual Delivery Date: 30/06/2023

Work Package/ Task: WP2/ T2.4

Document Owner: BSC

Contributors: BSC/ECMWF

Status: Final

CONFESS

Consistent representation of temporal variations of boundary forcings in reanalyses and seasonal forecasts

Research and Innovation Action (RIA)
H2020- LC-SPACE-18-EO-2020 Copernicus evolution: Research activities in support of the evolution of the Copernicus services - Copernicus Climate Change Service (C3S

Project Coordinator: Dr Magdalena Alonso Balmaseda (ECMWF)
Project Start Date: 01/11/2020
Project Duration: 36 months

Published by the CONFESS Consortium

Contact:
ECMWF, Shinfield Park, Reading, RG2 9AX, United Kingdom
Magdalena.Balmaseda@ecmwf.int

The CONFESS project has received funding from the European Union's Horizon 2020 research and innovation programme under grant agreement No 101004156.

Contents

Figures

Tables

1 Executive Summary

In order to study the potential impact of including time-varying aerosols from biomass burning in the ECMWF's seasonal forecasting system, idealised experiments were conducted based on selected test cases using climatological and observed emissions (so-called "perfect forecasts" of emissions). The emissions have been coupled with the Integrated Forecast System (IFS)'s model where aerosols interact with radiation which presents an important step towards including variable forcings in the seasonal forecast. An analysis of the forecast skill in these experiments shows that both versions of the interactive prognostic aerosols show mixed results, improving and degrading the scores for some variables with respect to a control forecast. The degraded performance is expected to be mitigated by tuning the atmospheric model to perform optimally with the aerosol fields.

Based on an analysis of extreme biomass burning events, three case studies have been selected (the Indonesian fire season of 2015, the fires in Australia in 2019/2020 and those in California in 2020) to evaluate the seasonal experiments. For these events we find changes in surface temperature and precipitation (only for the Indonesian 2015) in the seasonal hindcasts which use the observed and climatological biomass burning emissions. However these changes don’t always translate to an improved forecast of the events.

2 Introduction

2.1 Background

The impact of aerosol particles is widely recognized as an important factor for accurate climate and weather predictions. Proceeding from the idea that aerosol impacts manifest themselves more at the longer ranges than at the short/medium ranges Benedetti and Vitart (2018) have shown the potential of interactive prognostic aerosols to improve model prediction at the monthly timescales. A plausible physical mechanism behind this positive impact was hypothesised to be the aerosol modulation induced by the Madden-Julian Oscillation (MJO). For the extreme case of the Indonesian fires of 2015, the impact of the biomass burning aerosols was seen to persist at lead months 3 and 6, indicating potential for impact at the seasonal scales.

Biomass burning aerosols produced from agricultural practices in areas of Africa, South America and Indonesia have a recognized effect on climate. However, the temporal variations of these important aerosol species are not included in seasonal prediction systems which rather rely on fixed climatologies. In CONFESS we use the so-called IFS-COMPO model, a version of the ECMWF model where the atmosphere is coupled to the chemistry model used by CAMS (Copernicus Atmospheric composition Monitoring Service) via the radiation. We use the IFS-COMPO for runs at the seasonal scale with a reduced-resolution ensemble approach. Biomass burning emissions are prescribed with a climatology derived from the GFAS dataset as well as with observed emissions in re-forecast mode to establish a benchmark. This is the first time that a full time-varying biomass burning tracer is activated in a seasonal forecast configuration. The impacts are analysed for key cases such as the recent extended period of biomass burning in Australia (2019/2020), the 2015 fires in Indonesia and the 2020 fires in California. These extreme episodes are rare, but they may become more frequent in a changing climate and it is important to document their impact at the seasonal scale, particularly in the Tropics where they represent the largest contribution to aerosol load after dust.

Including for the first time a biomass burning aerosol in the ECMWF seasonal prediction system represents a huge step forward in the comprehensive and integrated representation of the Earth System. This allows us to understand the impact of extreme biomass burning events on regional seasonal prediction and represents a step forward in our capability to understand an important component of the Earth System such as the emissions from wildfires. This knowledge, coupled with the improvements in description of land and vegetation carried out in WP1, will also allow us to design a future service in which all components of the Copernicus services are harmoniously integrated. It will also develop a capability to respond to extreme events such as the recent Australian fires and to improve our preparedness to the long-term consequences of the most severe biomass burning events.

2.2 Scope of this deliverable

2.2.1 Objectives of this deliverable

In work package 2 a series of developments have been carried out to implement the capability of including biomass burning emissions in the ECMWF seasonal forecast system. This work aims to

implement and evaluate the impact of including biomass burning aerosols on the seasonal forecasting skill.

2.2.2 Work performed in this deliverable

- Create a climatology of observed biomass burning emissions from the CAMS Global Fire Assimilation System (GFAS).
- Implement observed and climatological biomass burning emissions in the ECMWF seasonal system.
- Define the case studies for the evaluation of including the observed emissions in the seasonal forecast system.
- Run seasonal ensemble experiments.
- Analyse the experiments with established metrics focusing on the biomass burning extreme events.

2.2.3 Deviations and counter measures:

The unavailability of the ECMWF MARS archive due to the migration of the computer facilities from Reading to Bologna impacted the access to the simulations which delayed the analysis of the simulations carried out by BSC.

3 ECMWF Seasonal Forecast System

3.1 The ECMWF's ENS system

Subseasonal forecasts out to 46 days have been produced routinely at ECMWF since March 2002 and operationally since October 2004 (Vitart, 2014). In the model version used in this study (CY47R3), which was operational between October 2021 and June 2023, the monthly forecasts are generated by extending the 15-day ensemble integrations to 46 days twice a week (at 0000 UTC on Mondays and Thursdays). Forecasts are based on the medium range/monthly ensemble forecast (ENS), which is part of the ECMWF's Integrated Forecast System. ENS includes 51 members run with a horizontal resolution of TCo639 (about 16 km) up to forecast day 15 and TCo319 (about 32 km) thereafter. The atmospheric model is coupled to an ocean model (NEMO) with a 1/4° horizontal resolution. For the CONFESS experiments, the forecast length has been extended to four months to cover the seasonal scale.

After a few days of model integrations, the model mean climate begins to differ from the initial conditions. No bias correction is applied to remove or reduce the drift in the model, and no steps are taken to remove or reduce any imbalances in the coupled model initial state. The effect of the drift on the model calculations is estimated a posteriori from integrations of the model in previous years (re-forecasts) and removed (calibration). The climatology that is provided by the re-forecasts is computed using a suite that includes only 11 members of 46-day integrations with the same configuration as the real-time forecasts, starting on the same day and month as the real-time forecast over the past 20 years. For the model integrations presented in this study, the re-forecasts are run with 25 ensemble members over a shorter period (2003–2021) due to the limited availability of the aerosol emissions.

Initial perturbations are generated using a combination of singular vectors and perturbations generated using the ECMWF ensemble of data assimilations, and model uncertainties are simulated using two stochastic schemes (Leutbecher et al. 2017). The aerosol fields are not perturbed in the different ensemble members. However, for natural aerosols such as desert dust and sea salt, whose emissions are parameterized based on meteorological variables—most prominently, winds—any perturbations on those will also reflect on perturbations on the aerosol emissions themselves.

3.2 The aerosol model

In the context of the Copernicus Atmosphere Monitoring Service (CAMS) and precursor projects, Global Earth-system Monitoring using Satellite and in-situ data (GEMS) and Monitoring Atmospheric Composition and Climate (MACC), ECMWF has developed a capability to monitor and forecast atmospheric composition, including aerosols, greenhouse gases, and reactive gases, using satellite observations and a combination of global and regional models. The atmospheric composition prediction system is based on the IFS meteorological model, maintained and developed by ECMWF. The version used in this work corresponds to cycle 47R3 of the IFS, for which a detailed description can be found on the ECMWF's web page (https://www.ecmwf.int/en/publications/ifs-documentation). Generally, IFS is not run with the full coupled chemistry due to its computational cost. Currently, the operational resolution of IFS with full chemistry is 40 km with 137 vertical levels up to 0.01 hPa, as opposed to the operational NWP without full chemistry, which has a resolution of

9 km but also 137 vertical levels up to 0.01 hPa. Aerosols are forecast within the global system by a bulk–bin scheme (Morcrette et al. 2009, Remy et al 2019), that includes seven species: dust, sea salt, black carbon, organic carbon, sulphates, secondary organic and nitrates. Dust aerosols are represented by three prognostic variables that correspond to three size bins, with bin limits of 0.03, 0.55, 0.9, and 20 µm in radius. Sea salt aerosols are also represented by three size bins with limits of 0.03, 0.5, 5, and 20 µm in radius. Emissions of natural aerosols such as desert dust and sea salt are parameterized based on model variables, with surface winds being the main driver. For all other tropospheric aerosols (carbonaceous aerosols and sulphates), emission sources are defined according to established inventories (Lamarque et al. 2010). Biomass burning emissions contributing to black carbon and organic matter loads are prescribed from the Global Fire Assimilation System (GFAS; Kaiser et al. 2012 which uses emissions estimated from the fire radiative power (FRP) provided by the MODIS instruments on board the Aqua and Terra satellite. This data set was used to create a biomass burning climatology over the years 2003-2021. Removal processes include sedimentation of all particles, wet and dry deposition, and in-cloud and below-cloud scavenging. For organic matter and black carbon, both the hydrophobic and hydrophilic components are considered. Overall, a total of 15 additional prognostic variables for the mass mixing ratio of the different components (bins or types) of the various aerosols are used in this configuration.

In the version of the global IFS used in this study, which is still in operation, the direct radiative effect of aerosols is taken into account using the aerosol climatology of Bozzo et al. (2020), which became operational after July 2017. In the experimental version of the system, however, the aerosol optical depth, which is then used to calculate the radiative impacts, can be computed directly from the mass mixing ratios of the prognostic aerosols provided by the aerosol module. We make use of this capability to set up experiments with the coupled Ensemble Prediction System, as described in the next section, to investigate the importance of the direct radiative impact of the prognostic aerosols relative to control runs that use the CAMS/Bozzo climatology for aerosol optical properties.

3.3 Experiments

Three experiments were run to assess the aerosol impacts (Table 1): one control integration with the climatological aerosols in which all settings are similar to the operational setup with 137 vertical levels, but at lower horizontal resolution (T255 corresponding to 80 km; hereafter CONTROL); an interactive prognostic aerosol run in which the prognostic aerosols are initialised using the time-varying CAMS reanalysis and climatological biomass burning emissions are used (PROG2); and a second interactive aerosol run in which the biomass burning emissions are daily observed values from GFAS (PROG1). Only the direct aerosol effect is taken into consideration, while indirect aerosol effects on clouds are not modelled. This could be a limitation of the current study.

We also note that the aerosol climatology used in the CONTROL experiment was derived from a previous version of the chemistry model, which has since then evolved. This implies that PROG2 and CONTROL have very different aerosol mean state, with implications for the coupling with radiation, impacting the general circulation of the atmosphere and the skill of the forecasts.

Prescribed emissions for the anthropogenic species over the years of interest (2003–2021) were used. Updating the emissions over the course of the re-forecasts is clearly essential, particularly for biomass burning emissions; these cannot be accounted for with persistence over the course of several weeks, as they have a natural life cycle of a few days. It is possible to take into account these emissions using

climatologies which is what we have done in PROG2. In PROG1 we have instead used the daily biomass burning emission. PROG1 represents a "best case scenario" because emissions are based on actual observations of MODIS FRP, but observed emissions are only available in re-forecast mode, and not when actually running a forecast. This where the biomass burning emission climatology can be used to introduce time-varying emissions in forecast mode. Ultimately, and ideally, if one had a prognostic model for biomass burning emissions related to weather parameters, the full impact of prescribing those important emissions versus modelling them could be assessed. This is still subject to much investigation, and it is not covered in this work/report.

For computational cost, the size of the ensemble was limited to 25 members plus one unperturbed forecast with a start date of September 1 over the period 2003-2021. Runs were set up to be 6 months long at a resolution of approximately 80x80km. The meteorological variables were initialised using ERA5 (Hersbach et al., 2020).

Table 1: Experimental set-up

Experiment	Description
CONTROL	Control experiment in which climatological aerosols are used (operational at ECMWF for the medium-range, monthly and seasonal prediction).
PROG1	experiment with fully interactive prognostic aerosols with observed daily biomass burning emissions from the GFAS database.
PROG2	experiment with fully interactive prognostic aerosols initialised with climatological biomass burning emissions, computed as an average over the years 2003-2021, from the GFAS database

3.4 Evaluation of Meteorological Scores

As part of the evaluation of the meteorological impact of the different configurations, the ECMWF's standard verification was run to produce monthly statistics. ERA5 is used as the verifying dataset. Scorecards show the difference in cumulative ranked probability skill scores (CRPSS) between two experiments for 20 different parameters (upper-air and surface fields) monthly means over the northern extratropics (north of 30°N) and the tropics (30°N–30°S band). Yellow and red colours (blue and cyan) indicate that the experiment being scored has lower (higher) CRPSS than the control experiment: the higher the CRPSS, the more skillful the experiment. A statistical test has been applied to the differences of CRPSS scores. It is based on a 10 000 resampling bootstrap procedure. Dark blue and dark red dots indicate that the difference of RPSS is statistically significant within the 5% level of confidence. The following variables are verified: total precipitation (tp), 2-meter temperature (t2m), surface temperature (stemp), sea surface temperature (sst), mean sea level pressure (mslp), temperature at 50 hPa (t50), horizontal wind at 50 hPa (u50), meridional wind at 50 hPa (v50), streamfunction at 200 hPa (sf200), velocity potential at 200 hPa (vp200), temperature at 200 hPa (t200), horizontal wind at 200 hPa (u200), meridional wind at 200 hPa (v200), geopotential at 500 hPa (z500), temperature at 500 hPa (t500), horizontal wind at 500 hPa (u500), meridional wind at 500 hPa (v500), temperature at 850 hPa (t850), horizontal wind at 850 hPa (u850), and meridional wind at 850 hPa (v850).

Interactive prognostic aerosol with observed biomass burning emissions (PROG1) have a large impact on the meteorological variables under consideration with respect to the climatological aerosols used in the CONTROL, but not always a positive one as shown in the left panel of Fig 3.4.1. The upper level temperature at 50hPa is negatively impacted as well as the horizontal wind at 50 hPa. On the other hand month 3 shows a significant improvement in upper level wind at 200 hPa at month 3. A similar configuration with a previous version of the aerosol model was tested in Benedetti and Vitart (2018). The authors found more positive impacts of the interactive prognostic aerosols with respect to the climatological aerosols. However, the model changes between model cycles were substantial, both in the treatment of the prognostic aerosols and in the aerosol climatology itself. Therefore a different outcome in the experiments is plausible. Results from the comparison of PROG1 and CONTROL are consistent with the findings by Benedetti and Vitart (2018) in that they confirm that the tropospheric aerosols have a profound the atmospheric circulation visible at early stages of the forecasts, affecting circulation patterns and their predictability, and therefore forecast skill.

Continuing with the analysis of the current experiment, PROG2 compared to CONTROL shows generally neutral behaviour. This is an encouraging result meaning that the climatological biomass burning emissions can be used in an interactive prognostic aerosol configuration without any significant degradation. This could be a basis for the inclusion of time-varying aerosols with climatological emission, which would allow one to run in full forecast mode, which is not possible if observed emissions are used.

A comparison of the two PROG experiments shows a positive impact of the prognostic aerosols when observed biomass burning emissions are used, especially true over the tropics. This results indicates that representing the interannual variability of the fires improves the forecast skill of large scale atmospheric variables over the Tropics. However, observed emissions can only be used in re-forecast mode, and therefore they are not a viable option for forecast mode.

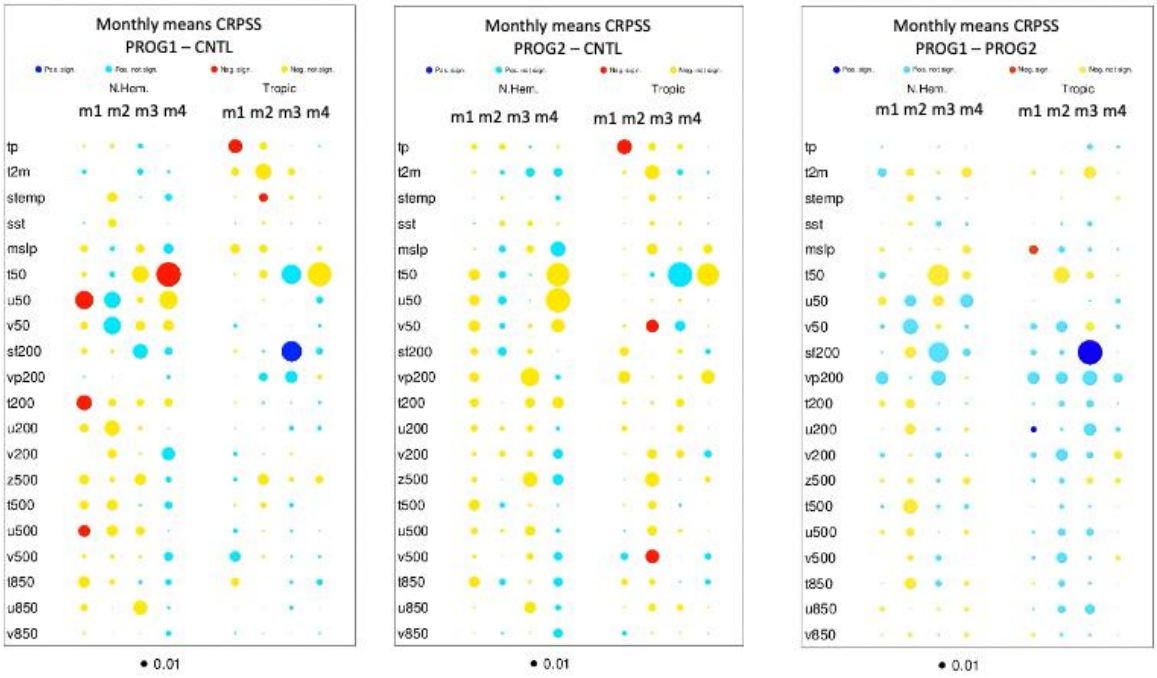

Figure 1. Scorecard for month 1-4 (North Hemisphere and Tropics) of PROG1 compared to CONTROL (left panel), PROG2 compared to CONTROL (middle panel) and PROG1 compared to PROG2 (right panel) for several meteorological variables. Blue dots indicate that the observed biomass burning emissions improve the forecasts at these lead times, while red dots indicate negative impact. Yellow and light blue dots represent negative and positive impact respectively which is not statistically significant.

4 Biomass Burning Case Studies

4.1 Defining the Case Studies

To evaluate further the impact of biomass burning emissions on the ECMWF seasonal forecast we have defined three case studies which correspond to the main wildfires that occurred during the last decade: Indonesia (2015), Australia (2019-2020) and California (2020). Figure 2 shows the wildfire flux of total carbon in aerosols from GFAS averaged over each of the regions. In these regions the wildfires are seasonal, occurring at the end of boreal summer and autumn, although for Australia it also extends to boreal winter. As indicated in red (and blue in the case of Australia) the wildfire flux of total carbon in aerosols for these three events was extraordinary compared to the climatology of other years.

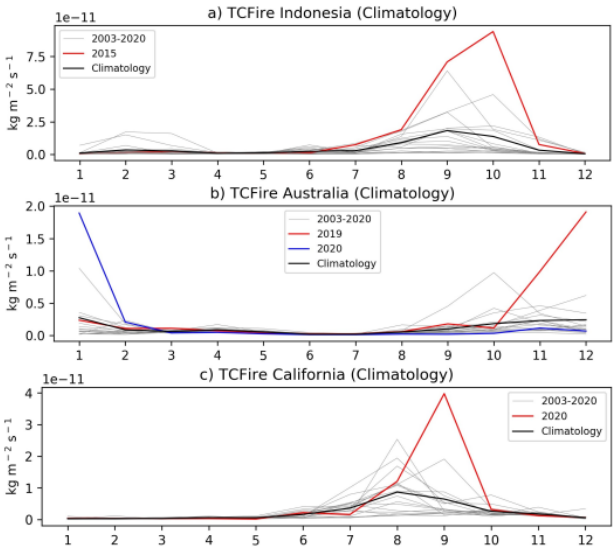

Figure 2. Annual timeseries of wildfire flux of total carbon in aerosols from CAMS for the three wildfires: a) Indonesia in 2015, b) Australia in 2019/2020, and c) California in 2020. The regions defined for each event are 8N-11S; 94E-126E for Indonesia, 18S-46S; 136E-167E for Australia, and 50N-30 N; 110W-130W for California. Grey lines are individual years in the period 2003-2021, the black line is the climatology, and the red/blue lines are the year of the event.

In Indonesia the fires were set during the dry season (July-October) of 2015 to clear land and remove agricultural residues that penetrated the sub-surface, inducing severe wildfires which burnt continuously until the return of the monsoon rains (Benedetti et al., 2016). The strength and prevalence of these fires is strongly influenced by large-scale climate patterns like El Niño, which in 2015 was exceptionally intense. This wildfire caused an environmental and public health catastrophe affecting the respiratory health of millions of people (Yin et al., 2020).

The 2019-2020 Australian wildfire season was singular in its severity and associated particulate emissions causing wide-scale smoke impacts across the southeast of the continent, leading to devastating consequences for lives, ecosystems, and property. This pollution remained in the atmosphere over New Zealand and South America for well over three months. Fasullo et al. (2021, 2023) showed that in response to the biomass aerosols over the Southern Hemisphere the surface

cooled, which impacted the tropical variability by shifting northward the intertropical convergence zone and cooling the sea surface temperature in the Niño3.4 region. They suggest the Australian fires may have had an important contribution to the 2020–2022 strong La Niña events. Moreover, the biomass burning emissions altered the terrestrial and marine biochemistry causing widespread phytoplankton blooms (Tang et al., 2021).

California in 2020 experienced a record of large fires due to the coalescence of multiple wildfires into fire complexes of massive size. The main driver of these fires was prolonged drought although management impacts on forest structure and fuel accumulation played an important role too (Goss et al., 2020).

4.2 Impact of Biomass Burning Emissions in the ECMWF Seasonal Forecasts

In this section we compare the seasonal hindcasts run by ECMWF to evaluate the impact of including interactive prognostic aerosols with the observed daily biomass burning emissions GFAS (PROG1) and with the climatological biomass burning emissions (PROG2). We focus on the three extreme biomass burning events and therefore we analyse hindcasts with initialised in September 2015, 2019 and 2020. Since PROG1 includes the observed time varying observed daily biomass burning emissions from GFAS we expect that the climate response to these events will be better represented in this experiment, while PROG2 provides the better approach for 'forecast mode', as the future emissions are unknown.

We note that the relative timing of the peak of the emissions and starting month of the forecast, as well as the geographical location and ongoing climate conditions, will have an impact on the results. Thus in 2015, the fires start in July and peak in October. By October the El Niño was well on its way, dominating the seasonal forecasts. Although the atmosphere is very sensitive to perturbations in the tropics, in the middle of El Niño the Indonesian fires will find it difficult to perturb the general circulation of the atmosphere. The situation is different for the 2019 Australian fires, which start in October and peak in December. By December the seasonal forecasts will have substantial spread, and the impact of fires will not be so easy to spot, especially since the emissions are not that large for this case. For the case of the 2020 California fires, the forecast initial dates are close to the peak of the emissions. It is an ideal scenario for impact regarding the timing. However, at mid-latitudes seasonal forecasts have lower signal-to-noise ratio, and the impact of the biomass burning is more difficult to detect.

4.2.1 Global Mean Response

Motivated by the results of Fasullo et al. (2021, 2023), who found that the biomass burning emissions from the 2020 Australia wildfires had a global imprint on surface temperature and precipitation, we start by analysing the global mean anomalies. Figure 3 shows the global mean top-of-atmosphere (TOA) shortwave flux, surface temperature and precipitation anomalies in each experiment. In this case we do not find a detectable impact on the global quantities (differences between the seasonal hindcasts are not statistically significant). We also computed the Northern Hemisphere and Southern Hemisphere means (not shown), since the aerosols may stay within a hemisphere, but again there is no evident impact from the biomass burning emissions.

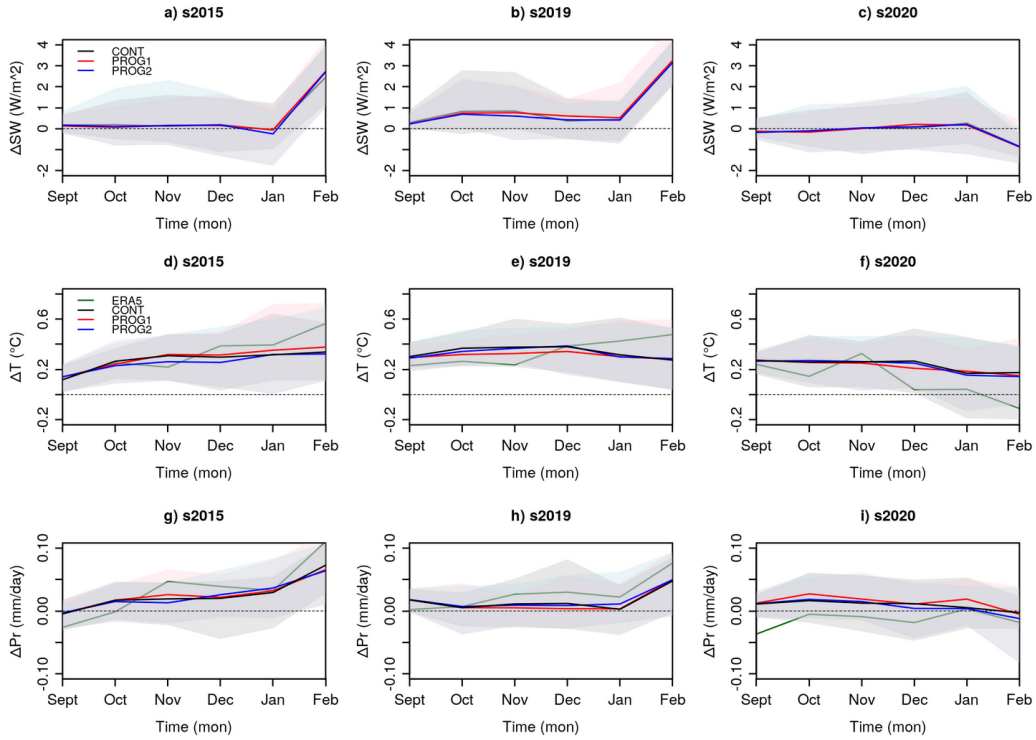

Figure 3. Global mean anomalies (with respect to 2003-2020) for top-of-atmosphere (TOA) shortwave flux (a-c), surface temperature (d-f) and precipitation (g-i) in the seasonal hindcasts (initialised in September) corresponding with the extreme biomass burning emission events. Shadings indicate the ensemble spread (min/max). For surface temperature and precipitation ERA5 (green line) has been included for comparison.

4.2.2 Regional Response

While no global impacts due to the biomass burning emissions are evident, we focus on the regions where the wildfires occurred to determine whether there are local impacts. We focus the analysis on the seasonal means: boreal Autumn (SON) and Winter (DJF).

4.2.2.1 Indonesia 2015:

Figure 4 shows the surface temperature differences among the seasonal forecasts for SON and DJF of 2015. Comparing the CONTROL with the PROG2 runs we find few significant differences in the regions where the fires occur in SON (figure 4a). In DJF we find that PROG2 is warmer than the CONTROL over several oceanic regions, with significant differences over the China and Arafura Seas (figure 4c). This warming is unlikely attributable to the climatological biomass burning emissions since we expect the opposite response. In contrast, comparing PROG1 and PROG2, we find lower surface temperatures in the regions where the wildfires occur in SON and extend over oceanic regions in DJF (figure 4b and d) in PROG1. This is evident over the islands of Borneo and Sumatra in SON, where the fires occur (figure 4b). This cooling is consistent with decreased solar radiation due to enhanced biomass burning emissions.

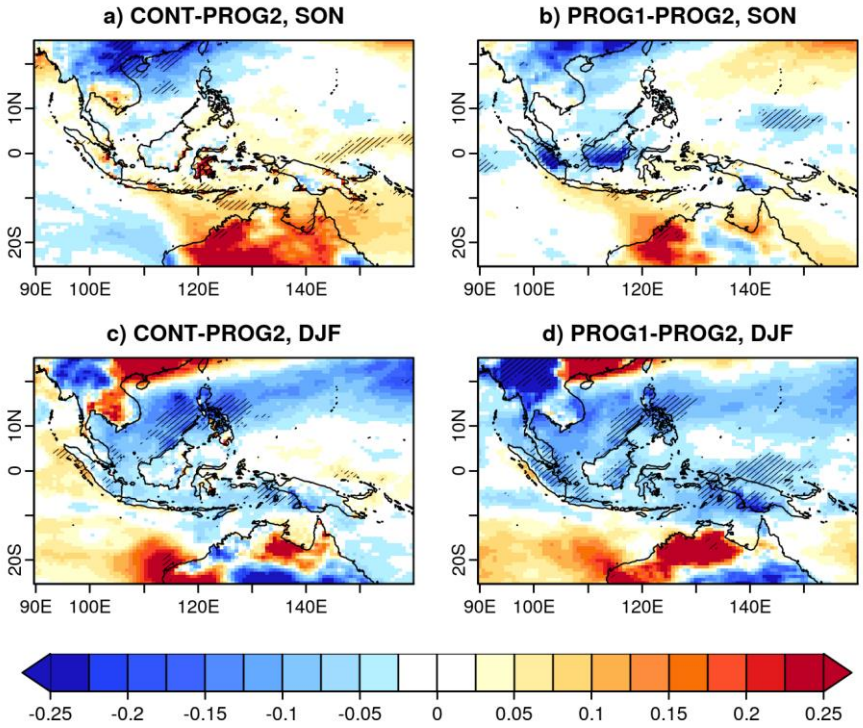

Figure 4. Seasonal surface temperature (°C) differences among the seasonal hindcasts experiments for the 2015 Indonesia wildfires. The hatching indicates statistically significant results according to a one-sided T-test at $p \leq 0.05$.

Figure 5 shows the precipitation differences among the seasonal experiments. Comparing the CONTROL and PROG2 we find some regional differences with enhanced and decreased precipitation but it is hard to determine whether these changes are due to the climatological biomass burning emissions alone. Comparing PROG1 and PROG2, in which the only difference is the biomass burning emissions, we find some regions with decreased precipitation in SON in PROG1 that resemble a southward shift. In DJF there are two bands with increased and decreased precipitation.

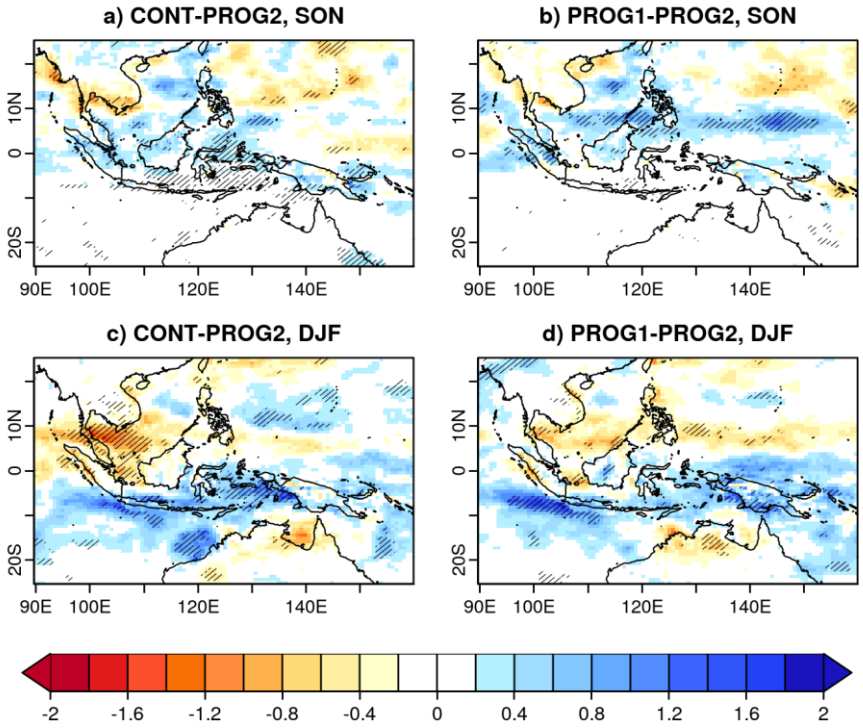

Figure 5. Seasonal precipitation (mm/day) differences among the seasonal hindcasts experiments for the 2015 Indonesia wildfires. The hatching indicates statistically significant results according to a one-sided T-test at $p \leq 0.05$.

To determine whether the differences on surface temperature and precipitation result in an improved forecast, we compare the forecast error against ERA5 in the three experiments for this event. Overall the forecast error in SON and DJF is very similar among the experiments. In SON the experiments tend to be warmer over the Maritime Continent and cooler to the north and south (figure 6a). In DJF the experiments are generally warmer (figure 6d). Comparing the errors in CONTROL and PROG2 we find small differences over the Maritime Continent in SON (figure 6b), as it can be inferred from the small differences shown in figure 4a. In DJF however, we find that over the Maritime Continent the error in PROG2 is greater than in the CONTROL, which suggests that forecast is degraded, at least for this event. Comparing PROG1 and PROG2, we find that the error in PROG1 is generally smaller in both SON and DJF. In SON including the observed biomass burning emissions results in lower temperatures over Borneo and Sumatra (where the fires occur) which are closer to ERA5 (figure 6c). In DJF, the cooler temperatures in PROG1 over the Maritime Continent result in a comparable forecast to CONTROL and improve the forecast over South East Asia (figure 6f).

For precipitation we again find that the forecast errors are very similar in the experiments (figure 7). We also find that generally the errors in PROG2 are larger than in the CONTROL (figure 7b,e). While PROG1 shows some improvements over PROG2 (around Sumatra and Java), the decreased precipitation over Philippines Sea results in greater errors in both SON and DJF.

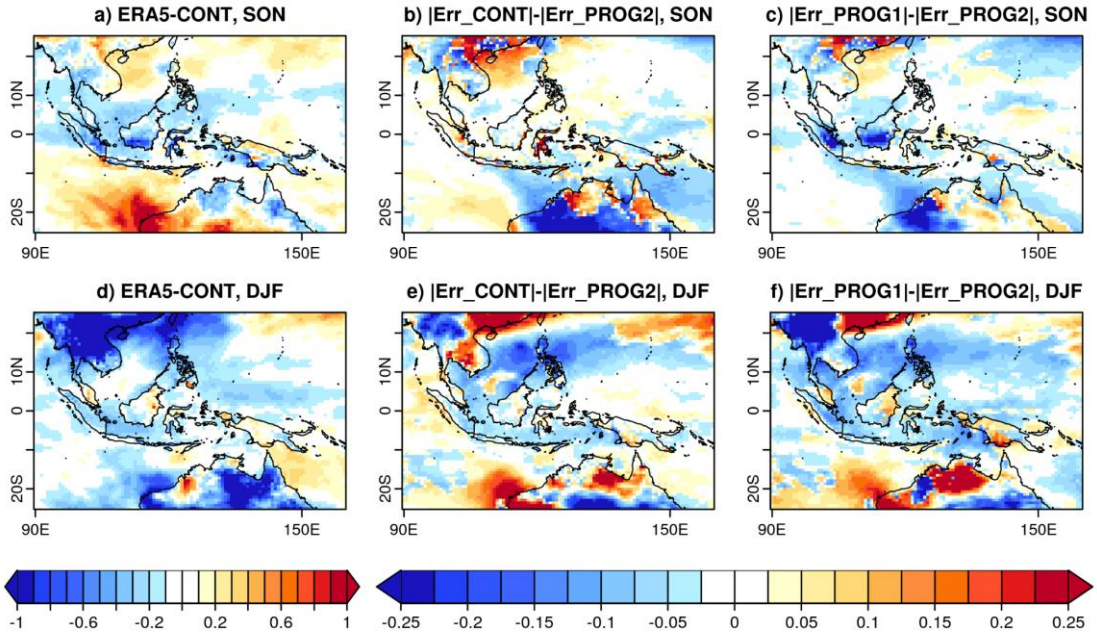

Figure 6. Surface temperature (°C) forecast error (ref: ERA5) in the ECMWF seasonal hindcast experiments for the 2015 Indonesia wildfires. Panels b,c,e,f show the differences in absolute error between experiments.

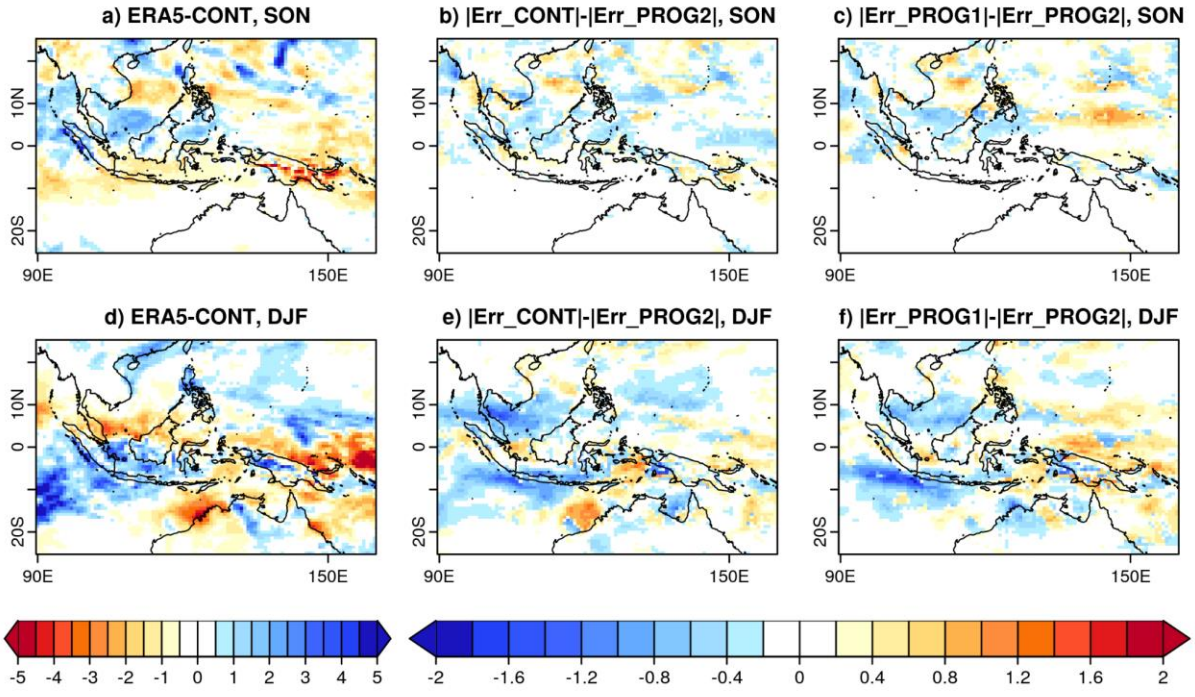

Figure 7. Precipitation (mm/day) forecast error (ref: ERA5) in the ECMWF seasonal hindcast experiments for the 2015 Indonesia wildfires. Panels b,c,e,f show the differences in absolute error between experiments.

4.2.2.2 Australia 2019/2020:

Figure 8 shows the surface temperature differences between the seasonal hindcasts for the 2019 startdate over Australia. Since the wildfire emissions peaked in December and January we focus on DJF, since the differences in the previous season are not expected to be due to the biomass burning emissions. Nonetheless figure 8a and c shows that there are some temperature differences among the experiments over Australia. In DJF we find few temperature differences between CONTROL and PROG2, but these are unlikely to be due to the biomass burning emissions due to the location (figure 8c). Comparing PROG1 and PROG2 we find few differences in surface temperature, although off the Southeastern coast of Australia where PROG1 is cooler than PROG2, which could be consistent with the effect expected from biomass burning emissions.

As for the previous case study, the forecast errors against ERA5 in the three hindcast experiments is comparable among them, and it is not evident whether a forecast is better than another (figure 9). It is worth noting however that the cooler anomalies simulated in PROG1 off the Southeastern coast of Australia result in an increased forecast error.

Changes in precipitation were also evaluated for this event but no relevant differences were found.

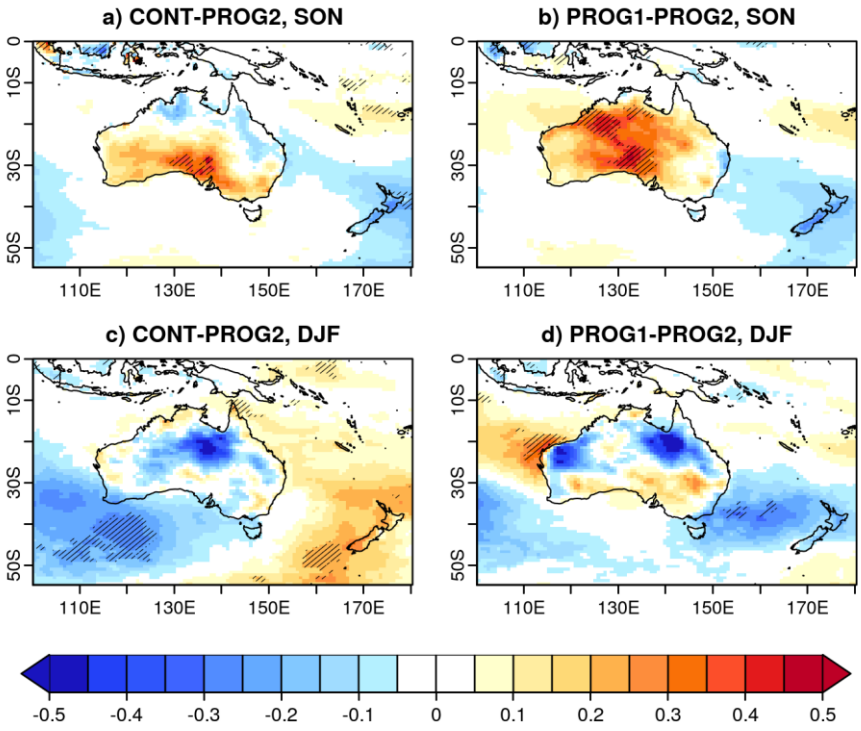

Figure 8. Seasonal surface temperature (°C) differences among the seasonal hindcasts experiments for the 2019 wildfires in Australia. The hatching indicates statistically significant results according to a one-sided T-test at $p \leq 0.05$.

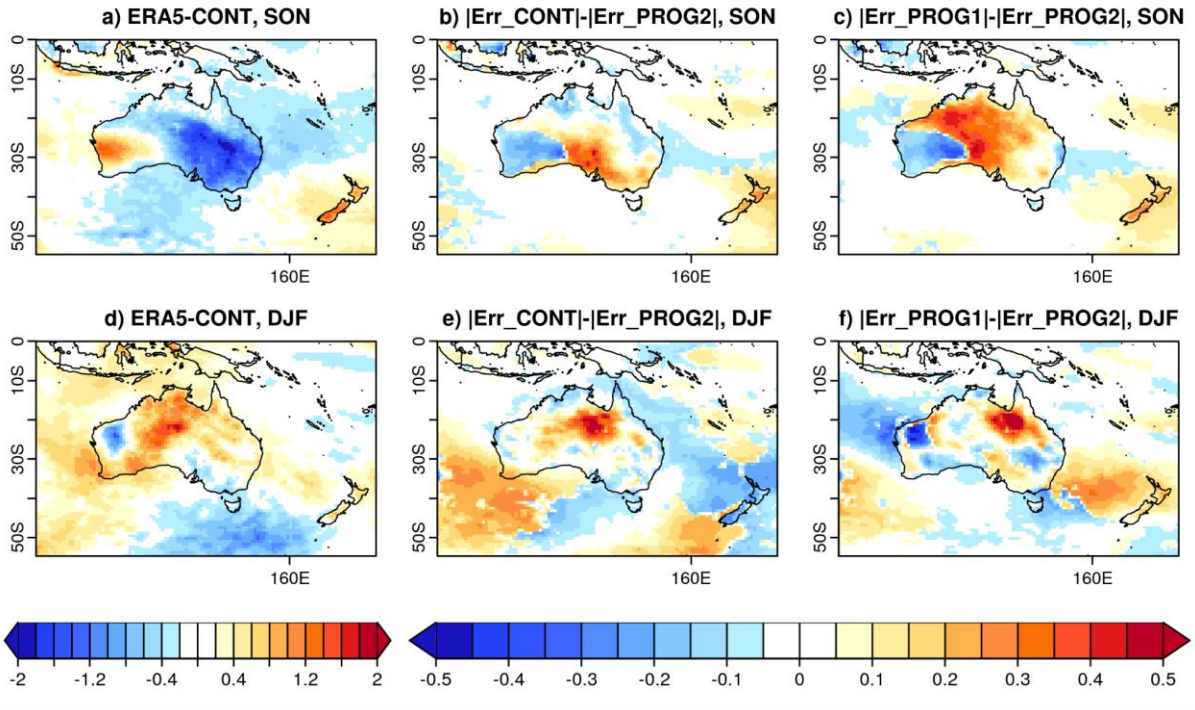

Figure 9. Surface temperature (°C) forecast error (ref: ERA5) in the ECMWF seasonal hindcast experiments for the 2019 Australian wildfires. Panels b,c,e,f show the differences in absolute error between experiments.

In contrast to the results shown in these hindcasts for the Australian 2019/2020 wildfire season, Fasullo et al. (2021, 2023) found much greater impacts, resembling a major Southern Hemisphere volcanic eruption. They found that the Southern Hemisphere and the Tropical Pacific SSTs cool and a northward displacement of the Intertropical Convergence Zone (ITCZ). None of these impacts have been found in these simulations. A possible reason might be that the IFS model does not include the indirect aerosol effects on clouds, which might be important for simulating such impacts.

4.2.2.3 California 2020:

Figure 10 shows the surface temperature differences between the seasonal hindcasts for the 2020 startdate over North America. The differences between CONTROL and PROG2 show no significant differences in SON (figure 10a), but in DJF the CONTROL is warmer than PROG2 over the central US (figure 10c). Comparing PROG1 and PROG2, we find that in SON PROG1 is cooler than PROG2 over the region where the California fires occur (figure 10b). Again consistent with the expected impact from the increased biomass burning emissions. In DJF however it is not evident whether the differences are due to the biomass emissions (figure 10d).

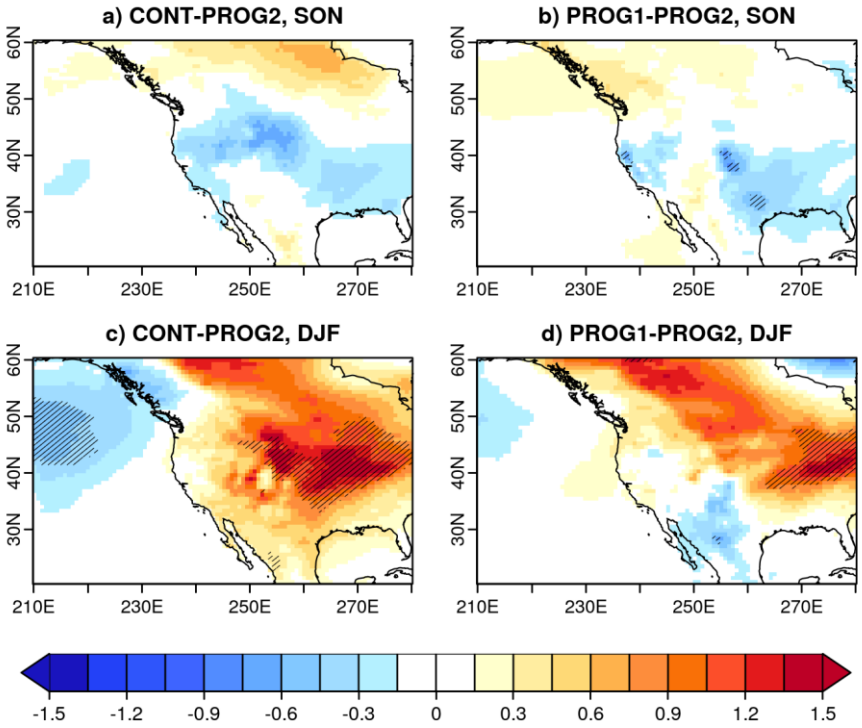

Figure 10. Seasonal surface temperature (°C) differences among the seasonal hindcasts experiments for the 2020 wildfires in California. The hatching indicates statistically significant results according to a one-sided T-test at $p \leq 0.05$.

As for the previous case studies, the forecast errors (against ERA5) for the California wildfires are comparable among the hindcast experiments (figure 11). We find a similar behaviour to the Indonesian wildfires case in DJF. Comparing CONTROL and PROG2 in DJF, the error in PROG2 is smaller over the US, while it is larger further North (figure 11e). PROG1 improves the errors over Canada and therefore provides a better forecast overall (figure 11f).

As in previous cases, we also evaluated the changes in precipitation but no relevant differences were found.

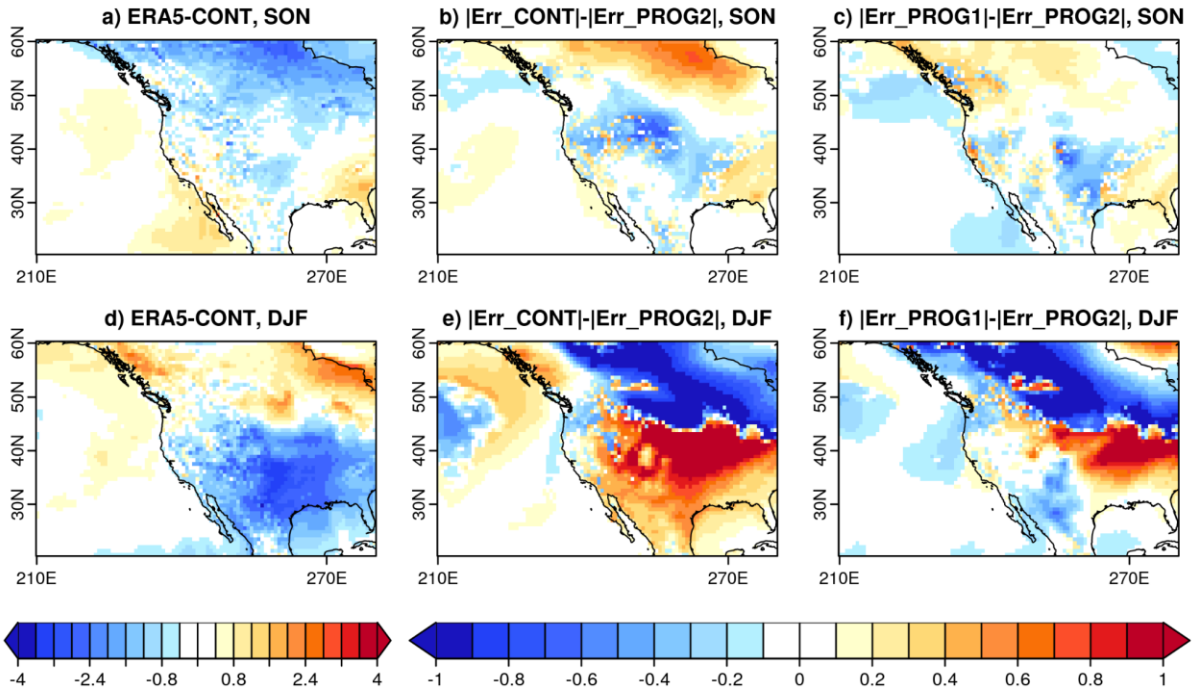

Figure 11. Surface temperature (°C) forecast error (ref: ERA5) in the ECMWF seasonal hindcast experiments for the 2020 wildfires in California. b,c,e,f show the differences in absolute error between experiments.

5 Summary and Conclusions

The work in CONFESS WP2 has led to a series of model developments to implement the capability of responding to biomass burning events. These developments include the creation of a climatology of observed biomass burning emissions from the CAMS Global Fire Assimilation System (GFAS) and the implementation of observed and the climatological biomass burning emissions in the IFS. To test these development a set of seasonal hindcasts experiments have been run: a control experiment in which climatological aerosols are used (CONTROL), an experiment with fully interactive prognostic aerosols with observed daily biomass burning emissions from the GFAS database (PROG1) and an experiment with fully interactive prognostic aerosols initialised with climatological biomass burning emissions, computed as an average over the years 2003-2021, from the GFAS database (PROG2).

The meteorological scores show mixed results. Both versions of interactive prognostic aerosols degrade the scores with respect to the CONTROL for some variables (50hPa temperature and winds) while improving others (200hPa winds). This is especially so when using observed emissions. While this might not seem an exciting result, it indicates that the aerosol fields have a noticeable impact on the atmospheric circulation. The degraded performance is likely due to the fact that the version of the atmospheric model has not been tuned to perform optimally with the aerosol fields used in PROG1 and PROG2. We would expect that a properly tuned model with interactive aerosols with climatological biomass burning emissions can be used for seasonal forecasts without detriment. This represents an important step towards including variable forcings in the seasonal forecast. A comparison with the “best case scenario” which is the experiment using observed emissions, shows some advantages of the latter. However observed emissions can only be used in hindcast mode as they would not be available in forecast mode. Ultimately a prognostic model for biomass emissions such as the one developed in this WP (see deliverable D2.2) would be needed to make more advances in this field.

To determine the impact of including the climatology and observed biomass burning emissions we have evaluated three case studies which correspond to the main wildfires that occurred during the last decade: Indonesia (2015), Australia (2019-2020) and California (2020). The main results are summarised as follows:

- For the Indonesia wildfires in 2015 we find differences in seasonal surface temperature and precipitation in the hindcasts which use the observed and climatological biomass burning emissions (PROG1 vs. PROG2). For this event, including the observed biomass burning emissions results in lower temperatures over Indonesia, especially over Borneo and Sumatra, resulting in an improvement of the forecast. In contrast the changes in precipitation seem to provide no improvement in the forecast.
- For the Australian wildfires in 2019/2020 we find lower surface temperature off the Southeastern coast of Australia when including the observed biomass burning emissions, however it does not improve the forecast. No impact on precipitation has been found.
- For the California wildfires in 2020 we find lower temperatures over the regions where the California wildfires occur when the observed biomass burning emissions are included, but it is not clear whether it improves the forecast. No impact on precipitation has been found.
- With few exceptions, it is not clear whether the seasonal hindcasts including the interactive prognostic aerosols forecast improve the response on seasonal surface temperature for these events with respect to the CONTROL hindcasts. One reason for this could be that the IFS model does not include the indirect aerosol effects on clouds, which may be important for simulating such impacts.

6 References

Benedetti et al. Atmospheric composition changes due to the extreme 2015 Indonesian fire season triggered by El Niño, BAMS State of the Climate, 2016.

Benedetti A. and F. Vitart, 2018: Can the Direct Effect of Aerosols Improve Subseasonal Predictability? Monthly Weather Review, Vol. 146, Issue 10, Page(s): 3481–3498, DOI: https://doi.org/10.1175/MWR-D-17-0282.1

Bozzo, A., Benedetti, A., Flemming, J., Kipling, Z., and Rémy, S., 2020. An aerosol climatology for global models based on the tropospheric aerosol scheme in the Integrated Forecasting System of ECMWF, Geosci. Model Dev., 13, 1007–1034, https://doi.org/10.5194/gmd-13-1007-2020.

Fasullo, J. T., Rosenbloom, N., Buchholz, R. R., Danabasoglu, G., Lawrence, D. M., & Lamarque, J.-F., 2021. Coupled climate responses to recent Australian wildfire and COVID-19 emissions anomalies estimated in CESM2. *Geophysical Research Letters*, 48, e2021GL093841

Fasullo, J. T., Rosenbloom, N., Buchholz, 2023. A multiyear tropical Pacific cooling response to recent Australian wildfires in CESM2.*Sci. Adv.*9, eadg1213.

Goss, M., Swain, D. L., Abatzoglou, J. T., Sarhadi, A., Kolden, C. A., Williams, A. P., & Diffenbaugh, N. S. (2020). Climate change is increasing the likelihood of extreme autumn wildfire conditions across California. *Environmental Research Letters*, 15(9), 094016.

Hersbach, H, Bell, B, Berrisford, P, et al. The ERA5 global reanalysis. *Q J R Meteorol Soc*. 2020; 146: 1999– 2049. https://doi.org/10.1002/qj.3803

Kaiser, J. W., Heil, A., Andreae, M. O., Benedetti, A., Chubarova, N., Jones, L., Morcrette, J.-J., Razinger, M., Schultz, M. G., Suttie, M., and van der Werf, G. R., 2012. Biomass burning emissions estimated with a global fire assimilation system based on observed fire radiative power, Biogeosciences, 9, 527–554, https://doi.org/10.5194/bg-9-527-2012.

Lamarque, J.-F., Bond, T. C., Eyring, V., Granier, C., Heil, A., Klimont, Z., Lee, D., Liousse, C., Mieville, A., Owen, B., Schultz, M. G., Shindell, D., Smith, S. J., Stehfest, E., Van Aardenne, J., Cooper, O. R., Kainuma, M., Mahowald, N., McConnell, J. R., Naik, V., Riahi, K., and van Vuuren, D. P., 2010. Historical (1850–2000) gridded anthropogenic and biomass burning emissions of reactive gases and aerosols: methodology and application, Atmos. Chem. Phys., 10, 7017–7039, https://doi.org/10.5194/acp-10-7017-2010.

Leutbecher, M., and Coauthors, 2017: Stochastic representations of model uncertainties at ECMWF: State of the art and future vision. *Quart. J. Roy. Meteor. Soc.*, 143, 2315–2339, https://doi.org/10.1002/qj.3094.

Morcrette, J.-J., and Coauthors, 2009: Aerosol analysis and forecast in the European Centre for Medium-Range Weather Forecasts Integrated Forecast System: Forward modeling. *J. Geophys. Res.*, 114, D06206, https://doi.org/10.1029/2008JD011235.

Rémy, S., Kipling, Z., Flemming, J., Boucher, O., Nabat, P., Michou, M., Bozzo, A., Ades, M., Huijnen, V., Benedetti, A., Engelen, R., Peuch, V.-H., and Morcrette, J.-J.: Description and evaluation of the tropospheric aerosol scheme in the European Centre for Medium-Range Weather Forecasts (ECMWF) Integrated Forecasting System (IFS-AER, cycle 45R1), Geosci. Model Dev., 12, 4627–4659, https://doi.org/10.5194/gmd-12-4627-2019, 2019.

Tang, J. Llort et al. Widespread phytoplankton blooms triggered by 2019-2020 Australian wildfires. Nature Vol. 597, 2021.

Vitart F. 2004. Monthly forecasting at ECMWF. *Mon. Weather Rev.* 132: 2761– 2779.

Vitart, F.: Evolution of ECMWF sub-seasonal forecast skill scores, Q. J. Roy. Meteorol. Soc., 140, 1889–1899, https://doi.org/10.1002/qj.2256, 2014.

Yin, S., X. Wang, M. Guo, H. Santoso, H. Guan, 2020. The abnormal change of air quality and air pollutants induced by the forest fire in Sumatra and Borneo in 2015. Atmosph. Res., 243 (2020), p. 105027, 10.1016/j.atmosres.2020.105027

Document History

Version	Author(s)	Date	Changes
First Draft	Roberto Bilbao (BSC), Angela Benedetti (ECMWF)	23/06/2023	
Final draft	Roberto Bilbao (BSC), Angela Benedetti (ECMWF)	30/06/2023	

Internal Review History

Internal Reviewers	Date	Comments
Name (Organisation)	dd/mm/yyyy	
Fransje van Oorschot (CNR-ISAC)	26/06/2023	Included in shared docs
Magdalena Alonso Balmaseda (ECMWF)	24/06/2023	Included in shared docs

Estimated Effort Contribution per Partner

Partner	Effort
ECMWF	2
BSC	4
Total	6